REPORT NO.
UCB/SEMM-93/12

STRUCTURAL ENGINEERING,
MECHANICS AND MATERIALS

A THICK PLATE FINITE ELEMENT WITH AN EXACT THIN LIMIT

by

FERDINANDO AURICCHIO

and

ROBERT L. TAYLOR

OCTOBER 1993

DEPARTMENT OF CIVIL ENGINEERING
UNIVERSITY OF CALIFORNIA
BERKELEY, CALIFORNIA

A THICK PLATE FINITE ELEMENT WITH AN EXACT THIN LIMIT

F.Auricchio R.L.Taylor

Department of Civil Engineering

University of California at Berkeley, Berkeley, CA 94720 USA

Abstract

We present a quadrilateral finite element developed within the framework of a shear deformable plate theory. The element takes advantage of internal rotational degrees of freedom (through the use of bubble functions) and a *linked* interpolation between the transverse displacement and the rotations (which guarantees higher order interpolation for the transverse displacement than for the rotations). A careful study of the element behavior is performed using an extensive set of mixed patch tests; results from several numerical examples also are presented. The element has proper rank and excellent interpolating capacity. Moreover, the element presents no locking effects at all; in fact, the shear energy may be set equal to zero (in a weak sense) without introducing any ill-conditioning in the problem, thus recovering a proper thin plate limit.

1 INTRODUCTION

In the development of a planar beam element within the context of Euler-Bernoulli (thin beam) theory, it is natural to introduce two degrees of freedom at each node (one transverse displacement and one rotation). Thus, as initially pointed out by Fraeijs de Veubeke [17], the condition of vanishing shear strain requires the rotation to be expressed as a derivative of the transverse displacement. Accordingly, the interpolation of the transverse displacement

must be of order higher than the one for the rotation. Such a condition may be fulfilled, for example, if the nodal rotation parameters are included in the approximation of the transverse displacement, i.e. if the transverse displacement field is *linked* to the nodal rotations through interpolation functions of order higher than the ones for the rotational field.

In the case of a thick beam independent interpolations for transverse displacement and rotations are assumed and the use of a linked interpolation leads to even more important properties, as presented in Reference [16, 36, 39] and reviewed in References [2]: a constant shear strain within the beam may be represented, hence avoiding locking effects in the limit thin case. Examples of two dimensional theories in which the displacement field is linked to the nodal rotational parameters can be found for the case of bending problems in the work of Greimann and Lynn [21], Lynn and Dhillon [26], Tessler and Hughes [40], Crisfield [13, 14, 15, 16] Xu [43, 44], Papadopoulos and Taylor [30].

While the use of a linked interpolation avoids locking in a thick beam formulation, it is not sufficient for a two dimensional plate. To avoiding locking, or equivalently to satisfy the mixed patch test, it is necessary to enrich the rotational field with extra modes, associated, for example, with internal bubble functions. The use of bubble functions to avoid an analogous locking in fluid-problems has also been recently investigated, as described in References [6, 11, 12]. Following this approach, several plate elements have already been presented based on a non-discrete description of the shear stress field [1, 2, 37, 53, 45]; however, as addressed in Reference [2], different pathologies are present in most of the elements developed to date, such as spurious modes or numerical sensitivity for the case of extremely thin plates. The latter problem may be partially avoided using an energy balancing method [18, 19].

In the present work we consider the interpolations for a four node quadrilateral element, which use internal modes for the rotations and linked interpolation for the transverse displacement. These interpolations lead to an element with none of the pathologies described previously. Thus, the element has the following characteristics:

- has a minimum number of internal degrees of freedom and thus is computationally efficient,
- passes *all* the patch tests,

- shows excellent interpolating capacity,
- solve exactly the thin plate limit case in a weak sense [1].

The paper is organized as follow. We start with a brief overview of the linear elastic shear deformable plate theory adopted. After that, we introduce a mixed finite element approximation together with the necessary interpolation requirements. We discuss a complete series of mixed patch tests which allows us to assess the quality of an interpolation scheme. We then describe the new finite element and present results from several numerical tests.

2 A LINEAR THICK PLATE THEORY

The development of a thick plate theory, which includes both bending deformation and the primary effects of transverse shear deformation, is commonly attributed to Mindlin [27] and Reissner [31]. The theory presented here is a simplification of the Mindlin-Reissner work and can be thought of a degeneration from the three-dimensional elasticity theory [52] or an example of a *direct approach* [20, 28, 32, 33].

Geometry and load

With the term *plate* we refer to a flat thin body, occupying the domain:

$$\Omega = \left\{ (x,y,z) \in \mathcal{R}^3 \;\mid\; z \in \left[-\frac{h}{2}, +\frac{h}{2} \right], (x,y) \in \mathcal{A} \subset \mathcal{R}^2 \right\}$$

where the plane $z = 0$ coincides with the middle surface of the undeformed plate and the transverse dimension, or *thickness* h, is small compared to the other two dimensions. Furthermore, loading $q(x,y)$ is restricted to the direction normal to the middle surface.

[1] In particular, as described later, the matrix from the shear energy may be set identically equal to zero without generating an ill-conditioned problem.

Kinematics

Limiting the discussion to the realm of infinitesimal kinematics, we assume that:

$$
\begin{aligned}
u(x,y,z) &= \quad z\theta_y(x,y) \\
v(x,y,z) &= -\ z\theta_x(x,y) \\
w(x,y,z) &= \quad w(x,y)
\end{aligned}
\tag{2.1}
$$

where u, v and w are the displacements along the x, y and z axes, respectively, and θ_x and θ_y are the rotations of the transverse line elements (initially perpendicular to the mid-surface) about the x and y axes. Accordingly, a straight line element, normal to the plate mid-surface in the undeformed configuration, remains straight, but not necessarily normal to the deformed mid-surface, allowing for transverse shear deformation. The basic kinematic ingredients are the curvature, $\mathbf{K}$, and the shear strain, $\boldsymbol{\Gamma}$, defined as:

$$
\begin{aligned}
\mathbf{K} &= \left\{ \begin{array}{c} \kappa_{xx} \\ \kappa_{yy} \\ \kappa_{xy} \end{array} \right\} = \left\{ \begin{array}{c} \theta_{y,x} \\ -\theta_{x,y} \\ \theta_{y,y} - \theta_{x,x} \end{array} \right\} \\
\boldsymbol{\Gamma} &= \left\{ \begin{array}{c} \gamma_{xz} \\ \gamma_{yz} \end{array} \right\} = \left\{ \begin{array}{c} \theta_y + w_{,x} \\ -\theta_x + w_{,y} \end{array} \right\}
\end{aligned}
$$

which can be expressed in terms of w and $\boldsymbol{\theta}$ as:

$$
\mathbf{K} = \mathbf{L}\boldsymbol{\theta} \quad , \quad \boldsymbol{\Gamma} = [\mathbf{e}\boldsymbol{\theta} + \nabla w]
$$

where:

$$
\mathbf{L} = \left[\begin{array}{cc} 0 & \dfrac{\partial}{\partial x} \\ -\dfrac{\partial}{\partial y} & 0 \\ -\dfrac{\partial}{\partial x} & \dfrac{\partial}{\partial y} \end{array} \right] \quad , \quad \mathbf{e} = \left[\begin{array}{cc} 0 & 1 \\ -1 & 0 \end{array} \right] \quad , \quad \nabla = \left\{ \begin{array}{c} \dfrac{\partial}{\partial x} \\ \dfrac{\partial}{\partial y} \end{array} \right\}
$$

with $\mathbf{L}$ and ∇ differential operators. As a consequence of the kinematic assumptions, we may distinguish between in-plane bending strains (ϵ_x, ϵ_y, γ_{xy}) and transverse shearing strains (γ_{xz}, γ_{yz}). In the thin plate theory

the transverse shearing strains are assumed to be zero, thus providing constraint equations, which permit θ_x and θ_y to be expressed as derivatives of the transverse displacement w. Conversely, in the thick plate theory we admit non-zero shear deformations.

Stresses and stress resultants

In the work presented here, for simplicity we assume that the normal stress in the z direction is negligible compared to the other stresses; hence:

$$\sigma_z = 0$$

Although this is inconsistent with a general three-dimensional theory and is not present in the work by Reissner (where σ_z varies through the thickness), it does not influence the development of a viable finite element formulation.

Consistent with the strain behavior, we may distinguish between in-plane stresses $(\sigma_x, \sigma_y, \tau_{xy})$ and transverse shearing stresses (τ_{xz}, τ_{yz}). Integration through the thickness defines the plate stress resultants per unit length:

$$M_x = \int_{-\frac{h}{2}}^{\frac{h}{2}} \sigma_x z dz \quad , \quad M_y = \int_{-\frac{h}{2}}^{\frac{h}{2}} \sigma_y z dz \quad , \quad M_{xy} = \int_{-\frac{h}{2}}^{\frac{h}{2}} \tau_{xy} z dz$$

$$S_x = \int_{-\frac{h}{2}}^{\frac{h}{2}} \tau_{xz} dz \quad , \quad S_y = \int_{-\frac{h}{2}}^{\frac{h}{2}} \tau_{yz} dz$$

For notational convenience, we collect the resultants as follow:

$$\mathbf{M} = \left\{ \begin{array}{c} M_x \\ M_y \\ M_{xy} \end{array} \right\} \quad , \quad \mathbf{S} = \left\{ \begin{array}{c} S_x \\ S_y \end{array} \right\}$$

Constitutive relation

Assuming the material to be homogeneous and linearly elastic, a plate constitutive relation may be written in terms of the resultant stresses and the kinematic variables as:

$$\left\{ \begin{array}{c} \mathbf{M} \\ \mathbf{S} \end{array} \right\} = \left[\begin{array}{cc} \mathbf{D}_B & \mathbf{0} \\ \mathbf{0} & \mathbf{D}_S \end{array} \right] \left\{ \begin{array}{c} \mathbf{K} \\ \boldsymbol{\Gamma} \end{array} \right\}$$

where, for isotropy:

$$\mathbf{D}_B = \frac{Eh^3}{12(1-\nu^2)} \begin{bmatrix} 1 & \nu & 0 \\ \nu & 1 & 0 \\ 0 & 0 & \frac{1}{2}(1-\nu) \end{bmatrix}$$

$$\mathbf{D}_S = kGh \begin{bmatrix} 1 & 0 \\ 0 & 1 \end{bmatrix} \quad , \quad G = \frac{E}{2(1+\nu)}$$

with E the Young 's modulus and ν the Poisson's ratio. Finally, k is a factor, introduced to correct the inconsistency through the thickness between the constant transverse shear strain, and the non-constant shear stress; k depends on the plate properties and is often set equal to 5/6 for homogeneous plates.

3 MIXED FINITE ELEMENT SOLUTION

As a starting point for the development of a mixed finite element scheme, we introduce the following functional, discussed in References [1, 2]:

$$\Pi(w, \boldsymbol{\theta}, \mathbf{S}) = \frac{1}{2} \int_A \left[\mathbf{K}^T(\boldsymbol{\theta}) \mathbf{D}_B \mathbf{K}(\boldsymbol{\theta}) \right] dA - \frac{1}{2} \int_A \left[\mathbf{S}^T \mathbf{D}_S^{-1} \mathbf{S} \right] dA + \int_A \left[\mathbf{S}^T (\nabla w + \mathbf{e}\boldsymbol{\theta}) \right] dA + \Pi_{ext}$$

where Π_{ext} describes the loads and the boundary effects. Following a *mixed* approach, we approximate the fields w, $\boldsymbol{\theta}$ and $\mathbf{S}$ with independent interpolation schemes; in particular we enrich the rotational field with internal degrees of freedom and link the transverse displacement field to the discrete rotational parameters. Accordingly we have:

$$\begin{aligned} w &= \mathbf{N}_w \hat{\mathbf{w}} + \mathbf{N}_{w\theta} \hat{\boldsymbol{\theta}} \\ \boldsymbol{\theta} &= \mathbf{N}_\theta \hat{\boldsymbol{\theta}} + \mathbf{N}_b \hat{\boldsymbol{\theta}}_b \\ \mathbf{S} &= \mathbf{N}_S \hat{\mathbf{S}} \end{aligned} \tag{3.1}$$

where:

$$\hat{\mathbf{w}} \ , \ \hat{\boldsymbol{\theta}}$$

are the degrees of freedom of the discretized system associated with the boundary nodes, while:

$$\hat{\boldsymbol{\theta}}_b \ , \ \hat{\mathbf{S}}$$

are respectively the internal rotational degrees of freedom and the shear stress degrees of freedom, and:

$$\mathbf{N}_w \ , \ \mathbf{N}_{w\theta} \ , \ \mathbf{N}_\theta \ , \ \mathbf{N}_b \ , \ \mathbf{N}_S$$

are sets of shape functions. Note that on a four-node quadrilateral element:

- $\mathbf{N}_b$ is zero on the boundary of the element, i.e. the internal rotational degrees of freedom are bubble modes,
- with an appropriate choice of the $\mathbf{N}_{w\theta}$ shape functions we are able to obtain a constant transverse shear strain along each side of the finite element,
- we guarantee a higher order interpolation for the complete polynomial in the transverse displacement than in the rotational field, as is required for the thin plate situation, when the rotations are simply the derivative of the displacements,
- we desire a transverse displacement interpolation with as few nodal parameters as possible and a larger number of rotational parameters, as required for the satisfaction of the mixed patch test.

After we introduce the interpolation scheme into Π, the stationary condition for the functional leads to the algebraic system:

$$\begin{bmatrix} \mathbf{0} & \mathbf{0} & \mathbf{0} & \mathbf{K}_{Sw}^T \\ \mathbf{0} & \mathbf{K}_{\theta\theta} & \mathbf{K}_{b\theta}^T & \mathbf{K}_{S\theta}^T \\ \mathbf{0} & \mathbf{K}_{b\theta} & \mathbf{K}_{bb} & \mathbf{K}_{bS} \\ \mathbf{K}_{Sw} & \mathbf{K}_{S\theta} & \mathbf{K}_{bS}^T & \mathbf{K}_{SS} \end{bmatrix} \begin{Bmatrix} \hat{\mathbf{w}} \\ \hat{\boldsymbol{\theta}} \\ \hat{\boldsymbol{\theta}}_b \\ \hat{\mathbf{S}} \end{Bmatrix} = \begin{Bmatrix} \mathbf{f}_w \\ \mathbf{f}_\theta \\ \mathbf{0} \\ \mathbf{0} \end{Bmatrix} \tag{3.2}$$

where $\mathbf{f}_w$ and $\mathbf{f}_\theta$ are the terms due to transverse load and boundary conditions, while:

$$\begin{aligned}
\mathbf{K}_{Sw} &= \int_A (\mathbf{N}_S)^T \nabla \mathbf{N}_w dA \\
\mathbf{K}_{\theta\theta} &= \int_A (\mathbf{L}\mathbf{N}_\theta)^T \mathbf{D}_B (\mathbf{L}\mathbf{N}_\theta) dA \\
\mathbf{K}_{b\theta} &= \int_A (\mathbf{L}\mathbf{N}_b)^T \mathbf{D}_B (\mathbf{L}\mathbf{N}_\theta) dA \\
\mathbf{K}_{S\theta} &= \int_A (\mathbf{N}_S)^T [\nabla \mathbf{N}_{w\theta} + \mathbf{e}\mathbf{N}_\theta] dA \\
\mathbf{K}_{bb} &= \int_A (\mathbf{L}\mathbf{N}_b)^T \mathbf{D}_B (\mathbf{L}\mathbf{N}_b) dA \\
\mathbf{K}_{bS} &= \int_A (\mathbf{e}\mathbf{N}_b)^T \mathbf{N}_S dA \\
\mathbf{K}_{SS} &= -\int_A \mathbf{N}_S^T \mathbf{D}_S^{-1} \mathbf{N}_S dA
\end{aligned}$$

If we first eliminate the internal rotational degrees of freedom and then the shear parameters, we get the following stiffness matrix, in terms of the external degrees of freedom:

$$\begin{bmatrix} -\mathbf{K}_{Sw}^T \mathbf{A}_{SS}^{-1} \mathbf{K}_{Sw} & -\mathbf{K}_{Sw}^T \mathbf{A}_{SS}^{-1} \mathbf{A}_{S\theta} \\ -\mathbf{A}_{S\theta}^T \mathbf{A}_{SS}^{-1} \mathbf{K}_{Sw} & \mathbf{A}_{\theta\theta} - \mathbf{A}_{S\theta}^T \mathbf{A}_{SS}^{-1} \mathbf{A}_{S\theta} \end{bmatrix} \begin{Bmatrix} \hat{\mathbf{w}} \\ \hat{\boldsymbol{\theta}} \end{Bmatrix} = \begin{Bmatrix} \mathbf{f}_w \\ \mathbf{f}_\theta \end{Bmatrix}$$

where:

$$\begin{aligned}
\mathbf{A}_{SS} &= \left[\mathbf{K}_{SS} - \mathbf{K}_{bS}^T (\mathbf{K}_{bb})^{-1} \mathbf{K}_{bS}\right] \\
\mathbf{A}_{S\theta} &= \left[\mathbf{K}_{S\theta} - \mathbf{K}_{bS}^T (\mathbf{K}_{bb})^{-1} \mathbf{K}_{b\theta}\right] \\
\mathbf{A}_{\theta\theta} &= \left[\mathbf{K}_{\theta\theta} - \mathbf{K}_{b\theta}^T (\mathbf{K}_{bb})^{-1} \mathbf{K}_{b\theta}\right]
\end{aligned}$$

Note that we are never required to invert $\mathbf{K}_{SS}$ alone, but are required to invert $\mathbf{A}_{SS}$; hence, we need only to guarantee its invertibility by an appropriate choice of the $\mathbf{N}_b$ interpolating functions. We desire $\mathbf{A}_{SS}$ to be invertible also for the case of $\mathbf{K}_{SS}$ identically equal to zero (i.e., we neglect the shear energy), which is a weak satisfaction of the thin plate limit. Accordingly, if such judicious choice of the $\mathbf{N}_b$ function is performed, then:

- we may always solve a sequence of problems converging to the thin plate case,

- depending on the purposes of the analysis, the shear energy may be arbitrarily included or excluded (setting $\mathbf{K}_{SS} = \mathbf{0}$), without the problem becoming ill-conditioned,
- we may always recover the shear parameters $\hat{\mathbf{S}}$, even for the case in which the shear energy is excluded.

It is interesting to observe that some of the elements presented in the literature [1, 37, 45, 49] should be re-investigate, taking into consideration the discussion of this section.

4 REQUIREMENTS FOR CONVERGENCE OF A MIXED FORMULATION

Convergence is the property by which the approximate solution obtained from a discrete scheme, such as a finite element model, approaches the exact solution for successive mesh refinements. *Consistency* and *stability* are sufficient requirements to imply convergence: consistency ensures that the discrete model reproduces the exact model for the limiting case of infinite number of degrees of freedom, while stability ensures that the solution of the discrete system is unique and not ill-conditioned.

Within a standard displacement finite element approach, the stability can be tested by checking that the stiffness matrix has appropriate rank, while consistency is verified by the patch test. The original patch test was introduced by Irons [9, 24] based on physical reasoning and established the capacity of the discrete model to exactly reproduce constant strain (curvature) states for simple patches of elements. Thereafter, other works have elaborated on the importance of the test, see for example References [25, 29, 35, 38, 42].

The convergence of a mixed finite element scheme is however more complex to verify and the mathematical conditions to be satisfied are embedded in the work of Babuska [3, 4] and Brezzi [10]. In a more physical framework, an extended version of the patch test viable for mixed formulations has been presented and discussed [47, 48, 50]. The two approaches seek to establish the stability of a mixed formulation.

In what follows, we describe a set of patch tests for a mixed finite element formulation of the thick plate theory.

- **Constant strain.** This is the original patch test and checks that the discrete formulation is able to reproduce exactly constant states for all the strain quantities involved in the functional. The satisfaction of this test guarantees consistency of the formulation and at the same time allows for a validation of the computer program. Accordingly, for a thick plate problem, the following states should be reproduced:

  - *Constant bending curvature.* The plate is clamped along one edge and subjected to constant bending moment along the opposite edge; all the rotations in the direction along which the bending occurs must be set to zero, to obtain a simple curvature (cylindrical) problem.
  - *Constant twisting curvature.* The plate is simply supported along two orthogonal edges and subject to constant edge twisting moments along the other two edges.
  - *Constant shear strain.* The plate is clamped along one edge and subjected to constant shear force along the opposite edge; all the rotations (including internal modes) are fixed in order to prevent bending.

  The patch test should be performed both on single element meshes and simple patches, with regular and non-regular element geometry (e.g., as shown in Figures 1-2). To investigate the *locking* in the limiting case of thin plates, it is important to perform all the described tests for the cases of a thick and a thin plate. Moreover, during the analyses it is convenient to keep the bending stiffness constant for the constant curvature test and the shear stiffness constant for the constant shear strain test [2], such that all cases return the same numerical results.

- **Counts of the degrees of freedom.** This part of the mixed patch test consists in checking some simple algebraic inequalities involving the number of unknowns. For the particular formulation presented here, the requirements are:

$$n_\theta + n_b + n_w \geq n_s \quad , \quad n_s \geq n_w \tag{4.1}$$

[2] To keep the bending stiffness constant the Young's modulus must be scaled proportional to $1/t^3$, while for keeping the shear stiffness constant it must be scaled by $1/t$.

where n_w, n_θ, n_b and n_s stand for the number of degrees-of-freedom for $\hat{\mathbf{w}}$, $\hat{\boldsymbol{\theta}}$, $\hat{\boldsymbol{\theta}}_b$ and $\hat{\mathbf{S}}$ respectively. The count conditions represent a necessary condition for the stability of the discrete problem, since they are necessary conditions for the solvability of the system 3.2.

These relations should be satisfied for any generic finite element mesh and usually are checked for different *patches* (including both single- and multi-element meshes, with a maximum or a minimum number of essential boundary conditions).

- **Eigen-analysis of the stiffness matrix.** The eigenvalues of the stiffness matrix are computed and the presence of zero eigenvalues in excess of the number of rigid body modes is assessed, since any excess modes indicate *rank-deficiency* (or zero energy modes). Again the analysis is performed for meshes (such as those shown in Figures 1-2) for the thick and thin plate. We note particularly that an eigenvalue should not tend to zero or infinity in the limiting thin case.

  The importance of this test is related to the fact that solving more general problems using rank-deficient elements can lead to instability in the solution and may result in non converging solutions (such as oscillations fluctuating around the exact solution) or occasionally in a singular global stiffness matrix. The presence of spurious zero eigenvalues at a multi-element level must be considered as an indication of ill-conditioned behavior and non-robustness of the formulation. If such singularity exists only for a single element, the issue is not so clear but still is not desirable.

5 A NEW THICK PLATE FINITE ELEMENT

We now describe a four node iso-parametric element and in the next section we show that the element passes all the patch tests and presents high accuracy for standard test problems. The bi-linear shape functions are used to map the parent domain in natural coordinates (ξ, η) to the real domain with coordinates (x, y); accordingly the quadrilateral region occupied by each

element may be expressed by:

$$\mathbf{x} = \sum_{i=1}^{4} N^i \mathbf{x}^i$$

where: $\mathbf{x} = \{x, y\}^T$ is any point in the element and $\mathbf{x}^i = \{x^i, y^i\}^T$ are the nodal coordinates; N^i are the bi-linear shape function:

$$N^i = \frac{1}{4}\left(1 + \xi^i \xi\right)\left(1 + \eta^i \eta\right)$$

with ξ^i and η^i being the values of the natural coordinates at node i (e.g., see References [22, 51]).

The transverse displacement interpolation is bi-linear in the nodal parameters $\hat{w}^i$, enriched with linked quadratic functions expressed in terms of the nodal rotations $\hat{\boldsymbol{\theta}}$:

$$w = \sum_{i=1}^{4} N^i \hat{w}^i - \sum_{i=1}^{4} N^i_{w\theta} L^i \left(\hat{\theta}^j_n - \hat{\theta}^i_n\right)$$

where L^i is the i-j side length, $\hat{\theta}^i_n$ and $\hat{\theta}^j_n$ are the components of the rotations of i and j nodes in the direction normal to the i-j side (Figure 3). The $N^i_{w\theta}$ shape functions are:

$$\mathbf{N}_{w\theta} = \left\{ \begin{array}{c} N^1_{w\theta} \\ N^2_{w\theta} \\ N^3_{w\theta} \\ N^4_{w\theta} \end{array} \right\} = \frac{1}{16} \left\{ \begin{array}{c} (1-\xi^2)(1-\eta) \\ (1+\xi)(1-\eta^2) \\ (1-\xi^2)(1+\eta) \\ (1-\xi)(1-\eta^2) \end{array} \right\}$$

The interpolation for the rotational field is bi-linear in the nodal parameters $\hat{\boldsymbol{\theta}}^i$, with added internal degrees of freedom $\hat{\boldsymbol{\theta}}_b$:

$$\boldsymbol{\theta} = \sum_{i=1}^{4} N^i \hat{\boldsymbol{\theta}}^i + \mathbf{N}_b \hat{\boldsymbol{\theta}}_b \tag{5.1}$$

where $\mathbf{N}_b$ are internal bubble functions. To construct $\mathbf{N}_b$, we adopt a backward approach; in fact, indicating with $\boldsymbol{\Gamma}_b$ the contribution to the shear strain from the internal rotational parameters, we first assume a convenient form

for $\mathbf{\Gamma}_b$ and then from $\mathbf{\Gamma}_b$ we derive the form of $\mathbf{N}_b$. Accordingly, in natural coordinates we choose:

$$\mathbf{\Gamma}_b = \begin{bmatrix} 1 & 0 & \eta & 0 \\ 0 & 1 & 0 & \xi \end{bmatrix} M_b \begin{Bmatrix} \hat{\theta}_b^1 \\ \hat{\theta}_b^2 \\ \hat{\theta}_b^3 \\ \hat{\theta}_b^4 \end{Bmatrix}$$

where $\hat{\theta}_b^j$ $(j = 1, .., 4)$ are parameter local to each element and $M_b = (1 - \xi^2)(1 - \eta^2)$ is a bubble function. Introducing the transformation discussed in Reference [34], the interpolation field in the mapped element may be expressed as:

$$\boldsymbol{\gamma}_b = \frac{j_o}{j} \mathbf{F}_o^{-T} \mathbf{\Gamma}_b$$

where:

- F_o is the jacobian of the iso-parametric mapping, evaluated at $\xi = \eta = 0$:
$$(F_o)_{i1} = \left.\frac{\partial x_i}{\partial \xi}\right|_{\xi=\eta=0} \quad , \quad (F_o)_{i2} = \left.\frac{\partial x_i}{\partial \eta}\right|_{\xi=\eta=0}$$
- j_o is the jacobian determinant evaluated at $\xi = \eta = 0$,
- j is the jacobian determinant.

Accordingly, we have:

$$\boldsymbol{\gamma}_b = \begin{bmatrix} F_{22} & -F_{12} & F_{22}\eta & -F_{12}\xi \\ -F_{21} & F_{11} & -F_{21}\eta & F_{11}\xi \end{bmatrix} \frac{M_b}{j} \hat{\boldsymbol{\theta}}_b$$

such that:

$$\mathbf{N}_b \hat{\boldsymbol{\theta}}_b = \mathbf{e}^{-1} \boldsymbol{\gamma}_b = \begin{bmatrix} F_{21} & -F_{11} & F_{21}\eta & -F_{11}\xi \\ F_{22} & -F_{12} & F_{22}\eta & -F_{12}\xi \end{bmatrix} \frac{M_b}{j} \hat{\boldsymbol{\theta}}_b$$

For the shear interpolation in natural coordinates we choose:

$$\mathbf{\Sigma} = \begin{bmatrix} 1 & 0 & \eta & 0 \\ 0 & 1 & 0 & \xi \end{bmatrix} \begin{Bmatrix} S^1 \\ S^2 \\ S^3 \\ S^4 \end{Bmatrix}$$

where S^j $(j = 1,..,4)$ are parameter local to each element. Again, following Reference [34], the interpolation field in the mapped element may be computed as:

$$\mathbf{S} = \mathbf{F}_o \Sigma$$

and we get:

$$\mathbf{S} = \begin{bmatrix} F_{11} & F_{21} & F^o_{11}\eta & F^o_{21}\xi \\ F_{12} & F_{22} & F^o_{12}\eta & F^o_{22}\xi \end{bmatrix} \begin{Bmatrix} S^1 \\ S^2 \\ S^3 \\ S^4 \end{Bmatrix}$$

Summarizing, the element has three external (global) degrees-of-freedom at each vertex i: the transverse displacement $\hat{w}_i$ and the two components of the rotation along the x-y coordinate axes, $\hat{\theta}^i_x$ and $\hat{\theta}^i_y$, respectively. In addition, it has four internal rotational degrees-of-freedom $\hat{\boldsymbol{\theta}}_b$ and four shear parameters $\hat{\mathbf{S}}$. Due to the fact that $\hat{\boldsymbol{\theta}}_b$ and $\hat{\mathbf{S}}$ are quantities local to each element, the matrix condensation presented in Section 4 may be performed at the element level. In the following we will refer to this new element as Q4-LIM (**Q**uadrilateral with **4** nodes, based on **LI**nked interpolation and **M**ixed approach).

We note that, due to the particular form of $\mathbf{N}_b$ and $\mathbf{N}_S$, the matrix $\mathbf{K}_{bS}$ may be integrated in closed form, is diagonal and given by:

$$\mathbf{K}_{bS} = \frac{6}{9} \begin{bmatrix} 1 & 0 & 0 & 0 \\ 0 & 1 & 0 & 0 \\ 0 & 0 & \frac{1}{5} & 0 \\ 0 & 0 & 0 & \frac{1}{5} \end{bmatrix} j_o$$

The integration for all the other stiffness matrices is performed numerically, using three integration points in each direction. For the results reported in the next section, the finite element load is consistent with the transverse displacement interpolation.

In closing the Section, we wish to note that a finite element with only two internal degrees of freedom has also been developed and presented in Reference [2]. This element has performances similar to the one presented here for thick plates. However, since only two internal rotations are introduced, $n_b < n_s$; thus, the thin plate case can be obtained only as a result of

a limiting process in which G goes to infinity and not directly as discussed in Section 3 and, thus, it does not possess an exact thin plate limit.

6 NUMERICAL EXAMPLES

The element described in Section 5 has been implemented into the Finite Element Analysis Program (FEAP) [51, 52] and its performance has been checked on the patch tests discussed in Section 4 and on several standard test problems.

The solutions obtained are compared with those from other elements available in the literature. In particular, we choose the triangular T3L [37], the quadrilateral Q4L [53] (both based on the use of internal rotational degrees of freedom and a linked interpolation for the transverse displacement), the quadrilateral T1 [22, 23] [3] and the quadrilateral DKQ [8]; the results reported for such elements are always obtained running the finest mesh for which results from the Q4-LIM element are presented. When available, analytical or series solutions are also reported.

6.1 Patch test: stability assessment

The Q4-LIM element has four internal rotational degrees of freedom and four shear parameters, accordingly $n_\theta = n_S$ and equation 4.1_1 is *a-priori* satisfied. The second algebraic requirement, i.e. equation 4.1_2, is checked on different meshes (including both single- and multi-element meshes, with a maximum or a minimum number of essential boundary conditions) and it is also always satisfied.

Since the constraint count is just a necessary condition for the stability of the formulation, an eigen-analysis on the stiffness matrix after condensation for patches of one or more elements (Figures 1-2) is performed, as described in Section 4. We consider a thick ($L/h = 10$), a thin ($L/h = 1000$) and a very thin plate ($L/h = 100000$); for the case of irregular meshes, the skewness parameter x/L is set equal to 0.2 (refer to Figures 1 and 2). The element always has the correct number of zero eigenvalues and no eigenvalue tends to zero or to infinity in the limit thin case.

[3] We recall that the T1 is identical to the Bathe-Dvorkin element described in Reference [7] for rectangular geometry.

In Tables 1-6 we report the eigenvalues for a single element test, both for the case with shear energy (Q4-LIMy) and for the case without shear energy (Q4-LIMn). Recalling that we keep the bending stiffness constant while reducing the thickness (going from the thick to the thin plate), it is noted that T1 has four eigenvalues which grow as the thickness is progressively reduced: these are the eigenvalues associated with the shear constraints imposed in the element. The presence of such growing eigenvalues indicates an inability of the T1 element to model the thin limit case, i.e. for a very thin plate numerical round-off dominates and the solution cannot be computed. On the other side, Q4-LIM has no growing eigenvalues; thus, as the thickness is reduced, the eigenvalues progressively tend to those obtained excluding the shear energy from the computation (Q4-LIMn).

6.2 Patch test: consistency assessment

To assess consistency, the ability to exactly reproduce constant strain states is tested on the meshes of Figures 1 and 2, for a thick and a thin case ($L/h = 10$ and $L/h = 1000$). To investigate possible pathologies in the limiting thin case, the bending stiffness is kept constant during the constant curvature test, while the shear stiffness is kept constant during the constant shear strain test.

The Q4-LIM element passes all the above consistency tests. To highlight other possible pathologies and to assess sensitivity to thickness and distorted shapes, we also perform eigen-analyses on patches. The Q4-LIM element is superior to other quadrilateral elements both for very thin plates and for distorted geometries.

6.3 Simply supported beam

In this example we test the ability of the element to perform analysis including or excluding the shear energy from the problem. We consider a very thick simply supported beam of length $L/h = 1$ with material properties given by:

$$E = 1000 \quad , \quad \nu = 0$$

The beam is constrained to produce cylindrical bending and is loaded in the middle of the span with a concentrated force $F = 400$ per unit length of

the cross section. Accordingly, denoting by $D = Eh^3/[12(1-\nu^2)]$ the plate bending stiffness and by $G = E/[2(1+\nu)]$ the shear stiffness, the vertical displacements due to bending and shear are given by:

$$w_b\left(\frac{L}{2}\right) = \frac{FL^3}{48D} = 0.10$$
$$w_s\left(\frac{L}{2}\right) = \frac{3}{10}\frac{FL}{Gh} = 0.24$$

for a total displacement of $w_{tot} = w_b + w_s = 0.34$. In Table 7, we report the numerical response of the Q4-LIM element in terms of vertical displacement, moment and shear for the case with and without shear energy, all quantities computed at the middle span of the beam. In Figure 4, we also plot the vertical displacement of the beam for both cases. It is noted that the element is able to converge either to the solution of the shear deformable theory or to the solution of the shear rigid theory, according to the inclusion or the exclusion of the shear energy, as discussed in Section 3. Again, we wish to stress that the thin plate solution is obtained without any numerical ill-conditioning of the system, contrary to the behavior of previously published work (e.g. [22, 23, 52]).

6.4 Square plate

A square plate is modeled using meshes of the type presented in Figure 5. Both a thick ($L/h = 10$) and a thin plate ($L/h = 1000$) are considered, where L is the side length and h the thickness, with load $q = 1$ and material properties:

$$E = 10.92 \quad , \quad \nu = 0.3$$

The numerical results for the simply supported square plate are presented in Tables 8, together with the Navier series solution [41]. Both the SS-1 and the SS-2 boundary conditions are considered for the thick plate (as discussed in References [22, 52]). To highlight the influence of the boundary condition on the plate response, contours for the twist moment M_{xy} are shown in Figures 6 and 7 for the thick plate with SS-1 and SS-2 boundary, respectively.

For a plate with no shear energy, we plot in Figure 8 the contour of the shear S_x obtained from a finite element analysis (left side) and from a

series solution (right side). It is evident that high accuracy for shears can be attained using the Q4-LIM element.

In Figure 9 we plot the vertical displacement for the SS-2 boundary condition for a wide range of thickness versus side length values. The results from the T1 element are also reported for comparison. The ability of the new element to analyze very thin plates is clearly evident.

The numerical results for the case of a clamped square plate are presented in Tables 9, together with series solutions for the thick case [46] and for the thin case. To compute the result for the thin plate, we performed an energy solution using:

$$w = \sum_{mn} a_{mn} \left[1 - \cos\left(\frac{m\pi x}{L}\right)\right] \left[1 - \cos\left(\frac{n\pi y}{L}\right)\right]$$

and a large number of terms.

6.5 Clamped circular plate

Also for the circular geometry (Figure 10) [4] two values of diameter D versus thickness h are considered to simulate a thick and a thin plate ($D/h = 10$ and $D/h = 100$). The load is $q = 1.0$ and the material properties are:

$$E = 10.92 \quad , \quad \nu = 0.3$$

The numerical results are presented in Table 10 and compared also with an analytical solution.

6.6 Simply supported skew plate

We consider a highly skewed plate ($\beta = 60^o$), simply supported along all boundaries. The plate has unit load q, side length $L = 100$ and two thicknesses are considered, e.g. $h = 1$ and $h = 0.1$. The material properties are:

$$E = 10.92 \quad , \quad \nu = 0.3$$

The displacement and the two principal bending moments at the center of the plate are reported in Table 11. In addition, in Table 12 we compare

[4] The mesh is generated using three blocks of elements and the central node has coordinate $(2.1R, 2.1R)$, where R is the radius of the plate.

the element performance in terms of energy, as suggested by Babuska and Scapolla [5]. The properties used are:

$$E = 3.0E7 \quad , \quad \nu = 0.3$$

with thickness $t = 0.01$, side length $L = 1$ and unit uniform load.

The excellent performance of our element on the skew plate problem is particularly noted.

CLOSURE

In the present paper we present a quadrilateral finite element developed within the framework of a shear deformable plate theory. The element takes advantage of internal degrees of freedom (for the rotational field) and *linked* interpolation, i.e. an explicit dependence of the transverse displacement on the discrete rotational field, to permit an exact (weak) thin plate limit without any locking behavior. The advantages of this interpolation can be summarized as follow:

- with an appropriate choice of the $\mathbf{N}_{w\theta}$ shape functions we are able to obtain a constant shear strain along each side of an element,
- we guarantee a higher order complete interpolation for the transverse displacement than for the rotational field, as is required for the thin plate situation, where the latter are simply the derivative of the former,
- we have a transverse displacement interpolation with as few nodal parameters as possible and we have a larger number of rotational parameters, as required for the satisfaction of the mixed patch test.

We present a careful evaluation of the element behavior, based on an extensive set of mixed patch tests. Moreover, the results for a group of standard numerical test problems are presented, together with the results from three other elements available in literature. The new element has proper rank, excellent accuracy and no locking effects in the limiting case of a thin plate; in fact, due to the particular order adopted for the condensation of the internal parameters, it is possible to include or exclude from the analysis the shear energy, recovering in the latter case a proper thin plate result.

References

[1] F. Auricchio and R.L. Taylor, *3-node triangular elements based on Reissner-Mindlin plate theory*, Report UCB/SEMM-91/04, Department of Civil Engineering, University of California at Berkeley, 1991, Copies available through NISEE. E-mail: nisee@cmsa.berkeley.edu.

[2] ———, *A new family of quadrilateral thick plate finite elements based on linked interpolation*, Report UCB/SEMM-93/10, Department of Civil Engineering, University of California at Berkeley, 1993, Copies available through NISEE. E-mail: nisee@cmsa.berkeley.edu.

[3] I. Babuska, *Error bounds for finite element methods*, Numerische Mathematik **16** (1971), 322–333.

[4] ———, *The finite element method with Lagrange multipliers*, Numerische Mathematik **20** (1973), 179–192.

[5] I. Babuska and T. Scapolla, *Benchmark computation and performance evaluation for rhombic plate bending problem*, International Journal for Numerical Methods in Engineering **28** (1989), 155–179.

[6] C. Baiocchi, F. Brezzi, and L.P. Franca, *Virtual bubbles and Galerkin-least-squares type methods (Ga.L.S.)*, Computer Methods in Applied Mechanics and Engineering **105** (1993), 125–141.

[7] K.J. Bathe and E.N. Dvorkin, *A four node plate bending element based on Reissner-Mindlin plate theory and mixed interpolation*, International Journal for Numerical Methods in Engineering **21** (1985), 367–383.

[8] J.L. Batoz and M.B. Tahar, *Evaluation of a new quadrilateral thin plate bending element*, International Journal for Numerical Methods in Engineering **18** (1982), 1655–1677.

[9] G.P. Bazeley, Y.K. Cheung, B.M.Irons, and O.C. Zienkiewicz, *Triangular elements in bending - conforming and non-conforming solution*, Proceeding of the Conference on Matrix Methods in Structural Mechanics (Wright-Paterson Air Force Base, Ohio), 1965.

[10] F. Brezzi, *On the existence, uniqueness and approximation of saddle point problems arising from Lagrange multipliers*, RAIRO **8** (1971), 129–151.

[11] F. Brezzi, M.O. Bristeau, L.P. Franca, M. Mallet, and G. Rogé, *A relationship between stabilized finite element methods and the Galerkin method with bubble functions*, Computer Methods in Applied Mechanics and Engineering **96** (1992), 117–129.

[12] F. Brezzi and M. Fortin, *Mixed and hybrid finite element methods*, vol. 15, Springer-Verlag, New York, 1991, Springer series in computational mathematics.

[13] M.A. Crisfield, *A four noded thin plate bending element using shear constraints - a modified version of Lyons' element*, Computer Methods in Applied Mechanics and Engineering **38** (1983), 93–120.

[14] ———, *A quadratic Mindlin element using shear constraints*, Computers & Stuctures **18** (1984), 833–852.

[15] ———, *Shear constraints and folded-plated structures*, Engineering Computations **2** (1985), 238–246.

[16] ———, *Finite elements and solution procedures for structural analysis*, vol. I: Linear analysis, Pineridge Press, Swansea, U.K., 1986.

[17] B. Fraeijs de Veubeke, *Displacement and equilibrium models in the finite element method*, Stress analysis (O.C. Zienkiewicz and G.S. Holister, eds.), John Wiley & Sons LTD, 1965.

[18] I. Fried, *Shear in C^o and C^1 bending finite elements*, International Journal of Solids and Structures **9** (1973), 449–460.

[19] ———, *Finite element analysis of incompressible material by residual energy balancing*, International Journal of Solids and Structures **10** (1974), 993–1002.

[20] A.E. Green and P.M. Naghdi, *On the derivation of shell theories by a direct approach*, Journal of Applied Mechanics **41** (1974), 173–176.

[21] L.F. Greimann and P.P. Lynn, *Finite element analysis of plate bending with transverse shear deformation*, Nuclear Engineering and Design **14** (1970), 223–230.

[22] T.J.R. Hughes, *The finite element method*, Prentice Hall, 1987.

[23] T.J.R. Hughes and T.E. Tezduyar, *Finite element based upon Mindlin plate theory with particular reference to the four node bilinear isoparametric element*, Journal of Applied Mechanics **48** (1981), 587–596.

[24] B.M. Irons, *Numerical integration applied to finite element methods*, Conf. on use of digital computers in structural engineering (University of Newcastle), 1966.

[25] B.M. Irons and A.Razzaque, *Experience with the patch test for convergence of finite element method*, Mathematical foundations of the finite element method (A.K. Aziz, ed.), Academic Press, 1972, pp. 557–587.

[26] P.P. Lynn and B.S. Dhillon, *Triangular thick plate bending elements*, First International Conference on Structural Mechanics in Reactor Technology (Berlin, Germany), 1971, p. M 6/5.

[27] R.D. Mindlin, *Influence of rotatory inertia and shear in flexural motion of isotropic, elastic plates*, Journal of Applied Mechanics **18** (1951), 31–38.

[28] P.M. Naghdi, *Finite deformation of elastic rods and shells*, Proceedings of the IUTAM Symposium on Finite Elasticity (Bethlehem PA) (D.E. Carlson and R.T. Shield, eds.), 1982, pp. 47–103.

[29] E.R. De Arantes Oliveira, *The patch test and the general convergence criteria of the finite element method*, International Journal of Solids and Structures **13** (1977), 159–178.

[30] P.Papadopoulos and R.L.Taylor, *A triangular element based on Reissner-Mindlin plate theory*, International Journal for Numerical Methods in Engineering **30** (1990), 1029–1049.

[31] E. Reissner, *The effect of transverse shear deformation on the bending of elastic plates*, Journal of Applied Mechanics **12** (1945), 69–76.

[32] J.C. Simo and D.D. Fox, *On a stress resultant geometrically exact shell model. Part I: formulation and optimal parametrization*, Computer Methods in Applied Mechanics and Engineering **72** (1988), 267–304.

[33] J.C. Simo, D.D. Fox, and M.S. Rifai, *On a stress resultant geometrically exact shell model. Part II: the linear theory, computational aspects*, Computer Methods in Applied Mechanics and Engineering **73** (1989), 53–92.

[34] J.C. Simo and M.S. Rifai, *A class of mixed assumed strain methods and the method of incompatible modes*, International Journal for Numerical Methods in Engineering **29** (1990), 1595–1638.

[35] G. Strang and G.J. Fix, *An analysis of the finite element method*, Prentice Hall, 1973.

[36] R.L. Taylor, *Finite element analysis of linear shell problems*, MAFELAP 1987: the mathematics of finite elements and applications VI (J. Whiteman, ed.), Academic Press, 1987.

[37] R.L. Taylor and F. Auricchio, *Linked interpolation for Reissner-Mindlin plate elements: Part II: a simple triangle*, International Journal for Numerical Methods in Engineering **36** (1993), 3057–3066.

[38] R.L. Taylor, J.C.Simo, O.C. Zienkiewicz, and C.H.Chan, *The patch test - a condition for assessing FEM convergence*, International Journal for Numerical Methods in Engineering **22** (1986), 39–62.

[39] A. Tessler and S.B. Dong, *On a hierarchy of conforming Timoshenko beam elements*, Computers & Structures **14** (1981), 335–344.

[40] A. Tessler and T.J.R. Hughes, *An improved treatment of transverse shear in the Mindlin-type four node quadrilateral element*, Computer Methods in Applied Mechanics and Engineering **39** (1983), 311–335.

[41] S. Timoshenko and S. Woinowsky-Krieger, *Theory of plates and shells*, second ed., McGraw Hill, New York, 1959.

[42] B. Fraeijs De Veubeke, *Variational principles and the patch test*, International Journal for Numerical Methods in Engineering **8** (1974), 783–801.

[43] Z. Xu, *A simple and efficient triangular finite element for plate bending*, Acta Mechanica Sinica **2** (1986), 185–192.

[44] ———, *A thick-thin triangular plate element*, International Journal for Numerical Methods in Engineering **33** (1992), 963–973.

[45] Z. Xu, O.C. Zienkiewicz, and L.F. Zeng, *Linked interpolation for Reissner-Mindlin plate elements: Part III: an alternative quadrilateral*, International Journal for Numerical Methods in Engineering (1993), to appear.

[46] Cao Zhiyuan and Yang Shengtian, *Theory and applications of thick dynamics*, Science Press, 1983, in Chinese.

[47] O.C. Zienkiewicz and D.Lefebvre, *Three-field mixed approximation and the plate bending problem*, Communications in Applied Numerical Methods **3** (1987), 301–309.

[48] ———, *Mixed methods for F.E.M. and the patch test: some recent development*, Analyse Mathematique et Applications, Gauthier-Villars, 1988.

[49] _____, *A robust triangular plate bending element of Reissner-Mindlin type*, International Journal for Numerical Methods in Engineering **26** (1988), 1169–1184.

[50] O.C. Zienkiewicz, S.Qu, R.L.Taylor, and S.Nakazawa, *The patch test for mixed formulation*, International Journal for Numerical Methods in Engineering **23** (1986), 1873–1883.

[51] O.C. Zienkiewicz and R.L. Taylor, *The finite element method*, fourth ed., vol. I, McGraw Hill, New York, 1989.

[52] _____, *The finite element method*, fourth ed., vol. II, McGraw Hill, New York, 1991.

[53] O.C. Zienkiewicz, Z. Xu, L.F. Zeng, A. Samuelsson, and N.E. Wiberg, *Linked interpolation for Reissner-Mindlin plate elements: Part I: a simple quadrilateral*, International Journal for Numerical Methods in Engineering **36** (1993), 3043–3056.

Q4-LIMy	5.8593E+00	5.8593E+00	4.2448E+00	2.2601E+00	1.3000E+00	7.0000E-01
	2.9671E-01	2.9671E-01	4.3837E-02	8.8113E-16	1.5694E-16	-2.6733E-17
Q4-LIMn	6.1808E+00	6.1808E+00	4.7054E+00	2.4500E+00	1.3000E+00	7.0000E-01
	2.9690E-01	2.9690E-01	4.4630E-02	-7.3144E-16	3.6991E-16	-9.0807E-17
T1	9.1000E+01	9.1000E+01	3.2149E+01	2.9167E+01	1.3000E+00	7.0000E-01
	4.5000E-01	4.5000E-01	5.0805E-02	8.2750E-15	-5.3812E-15	3.3604E-16
DKQ	3.1546E+00	3.1546E+00	1.4839E+00	1.3000E+00	7.7000E-01	7.0000E-01
	4.1539E-01	4.1539E-01	5.1702E-02	-4.2142E-16	-1.6669E-16	-7.2268E-17

Table 1: Eigenvalues for thick regular mesh ($L/t = 10$)

Q4-LIMy	6.5198E+00	5.4670E+00	4.3822E+00	2.3472E+00	1.3300E+00	6.8829E-01
	3.1870E-01	2.7508E-01	4.0391E-02	-9.0475E-16	-3.2150E-16	-3.2966E-17
Q4-LIMn	6.8726E+00	5.7288E+00	4.8333E+00	2.5300E+00	1.3302E+00	6.8858E-01
	3.1890E-01	2.7524E-01	4.1066E-02	-6.5560E-16	5.6487E-16	1.3975E-17
T1	1.0118E+02	9.9528E+01	3.5361E+01	3.2498E+01	1.3282E+00	6.8962E-01
	4.8377E-01	4.2317E-01	4.6886E-02	3.4031E-15	2.4513E-15	-2.0133E-15
DKQ	3.5401E+00	2.7958E+00	1.4726E+00	1.3258E+00	7.6551E-01	6.8640E-01
	4.3544E-01	3.9889E-01	4.7468E-02	2.0612E-16	-1.7057E-16	-2.7072E-17

Table 2: Eigenvalues for thick irregular mesh ($L/t = 10$)

Q4-LIMy	6.1808E+00	6.1808E+00	4.7053E+00	2.4500E+00	1.3000E+00	7.0000E-01
	2.9690E-01	2.9690E-01	4.4630E-02	3.1852E-16	-1.8473E-16	-6.2348E-17
Q4-LIMn	6.1808E+00	6.1808E+00	4.7054E+00	2.4500E+00	1.3000E+00	7.0000E-01
	2.9690E-01	2.9690E-01	4.4630E-02	-7.3144E-16	3.6991E-16	-9.0807E-17
T1	9.1000E+05	9.1000E+05	3.1500E+05	2.9167E+05	1.3000E+00	7.0000E-01
	4.5000E-01	4.5000E-01	5.1852E-02	-4.4830E-11	-2.2291E-11	3.7136E-12
DKQ	3.1546E+00	3.1546E+00	1.4839E+00	1.3000E+00	7.7000E-01	7.0000E-01
	4.1539E-01	4.1539E-01	5.1702E-02	-4.2142E-16	-1.6669E-16	-7.2268E-17

Table 3: Eigenvalues for thin regular mesh ($L/t = 1000$)

Q4-LIMy	6.8725E+00	5.7287E+00	4.8332E+00	2.5300E+00	1.3302E+00	6.8858E-01
	3.1890E-01	2.7524E-01	4.1066E-02	-4.8957E-16	-2.9995E-16	5.6809E-17
Q4-LIMn	6.8726E+00	5.7288E+00	4.8333E+00	2.5300E+00	1.3302E+00	6.8858E-01
	3.1890E-01	2.7524E-01	4.1066E-02	-6.5560E-16	5.6487E-16	1.3975E-17
T1	1.0117E+06	9.9527E+05	3.4712E+05	3.2484E+05	1.3284E+00	6.8979E-01
	4.8383E-01	4.2318E-01	4.7761E-02	9.9054E-11	4.5190E-12	3.5108E-12
DKQ	3.5401E+00	2.7958E+00	1.4726E+00	1.3258E+00	7.6551E-01	6.8640E-01
	4.3544E-01	3.9889E-01	4.7468E-02	2.0612E-16	-1.7057E-16	-2.7072E-17

Table 4: Eigenvalues for thin irregular mesh ($L/t = 1000$)

Q4-LIMy	6.1808E+00	6.1808E+00	4.7054E+00	2.4500E+00	1.3000E+00	7.0000E-01
	2.9690E-01	2.9690E-01	4.4630E-02	-6.1035E-16	1.7055E-16	1.9840E-17
Q4-LIMn	6.1808E+00	6.1808E+00	4.7054E+00	2.4500E+00	1.3000E+00	7.0000E-01
	2.9690E-01	2.9690E-01	4.4630E-02	-7.3144E-16	3.6991E-16	-9.0807E-17
T1	9.1000E+09	9.1000E+09	3.1500E+09	2.9167E+09	1.3000E+00	7.0000E-01
	4.5000E-01	4.5000E-01	5.1852E-02	-1.4452E-07	1.4444E-07	1.1585E-07
DKQ	3.1546E+00	3.1546E+00	1.4839E+00	1.3000E+00	7.7000E-01	7.0000E-01
	4.1539E-01	4.1539E-01	5.1702E-02	4.5723E-16	9.6889E-17	-6.7714E-17

Table 5: Eigenvalues for extremely-thin regular mesh ($L/t = 100000$)

Q4-LIMy	6.8726E+00	5.7288E+00	4.8333E+00	2.5300E+00	1.3302E+00	6.8858E-01
	3.1890E-01	2.7524E-01	4.1066E-02	-8.6204E-16	-7.5921E-16	1.3324E-17
Q4-LIMn	6.8726E+00	5.7288E+00	4.8333E+00	2.5300E+00	1.3302E+00	6.8858E-01
	3.1890E-01	2.7524E-01	4.1066E-02	-6.5560E-16	5.6487E-16	1.3975E-17
T1	1.0117E+10	9.9527E+09	3.4712E+09	3.2484E+09	1.3284E+00	6.8979E-01
	4.8383E-01	4.2318E-01	4.7761E-02	6.3630E-07	-1.4301E-07	-7.5890E-08
DKQ	3.5401E+00	2.7958E+00	1.4726E+00	1.3258E+00	7.6551E-01	6.8640E-01
	4.3544E-01	3.9889E-01	4.7468E-02	5.3399E-16	1.0328E-16	5.7238E-17

Table 6: Eigenvalues for extremely-thin irregular mesh ($L/t = 100000$)

	Q4-LIM					T1	
Mesh	w_b	w_s	w_{tot}	M	S	w_{tot}	M
1×10	0.99889	2.40001	3.3989	950	200	3.3975	950
1×50	0.99993	2.39997	3.3999	990	200	3.3999	990
1×100	1.00000	2.40000	3.4000	995	200	3.4000	995
Ex.sol.	1.00000	2.40000	3.4000	995	200	3.4000	995

Table 7: Simply supported beam.

	THICK (SS1)		THICK (SS2)		THIN (SS2)	
Mesh	w / $(\frac{qL^4}{100D})$	M / $(\frac{qL^2}{100})$	w / $(\frac{qL^4}{100D})$	M / $(\frac{qL^2}{100})$	w / $(\frac{qL^4}{100D})$	M / $(\frac{qL^2}{100})$
2 x 2	0.43261	4.6805	0.42626	4.4686	0.40365	4.4675
4 x 4	0.45629	4.9597	0.42720	4.7099	0.40586	4.7103
8 x 8	0.45883	5.0484	0.42727	4.7690	0.40616	4.7690
16 x 16	0.46077	5.0821	0.42728	4.7837	0.40622	4.7837
32 x 32	0.46144	5.0922	0.42728	4.7874	0.40623	4.7874
T3L	0.46084	5.0900	0.42718	4.7892	0.40615	4.7875
Q4L	0.46179	5.0963	0.42729	4.7884	0.40623	4.7884
T1	0.46127	5.0904	0.42726	4.7868	0.40621	4.7868
Series	-	-	0.42728	4.7886	0.40624	4.7886

Table 8: Simply supported square plate: displacement and moment at the center. Thick plate: $L/h = 10$. Thin plate: $L/h = 1000$.

	THICK		THIN	
Mesh	w / $(\frac{qL^4}{100D})$	M / $(\frac{qL^2}{100})$	w / $(\frac{qL^4}{100D})$	M / $(\frac{qL^2}{100})$
2 x 2	0.14211	1.8108	0.11469	1.7311
4 x 4	0.14858	2.1968	0.12362	2.1629
8 x 8	0.14997	2.2889	0.12584	2.2590
16 x 16	0.15034	2.3122	0.12637	2.2827
32 x 32	0.15043	2.3180	0.12649	2.2886
T3L	0.15038	2.3173	0.12643	2.2880
Q4L	0.15044	2.3195	0.12650	2.2900
T1	0.15044	2.3191	0.12651	2.2897
Series	0.1499	2.31	0.12653	2.2905

Table 9: Clamped square plate: displacement and moment at the center. Thick plate: $L/h = 10$. Thin plate: $L/h = 1000$.

	THICK		THIN	
Mesh	w	M	w	M
1	42.191	4.8010	40576	4.7980
2	41.760	5.0682	40027	5.0670
4	41.641	5.1337	39881	5.1335
8	41.610	5.1505	39844	5.1505
16	41.602	5.1548	39835	5.1548
T3L	41.597	5.1545	39829	5.1549
Q4L	41.602	5.1548	39835	5.1548
T1	41.586	5.1540	39819	5.1540
Ex.sol.	41.599	5.1563	39831	5.1563

Table 10: Simply supported circular plate: displacement and moment at the center. Thick plate: $D/h = 10$. Thin plate: $D/h = 100$.

	THICK			THIN		
Mesh	w / $(\frac{qL^4}{100D})$	M_1 / $(\frac{qL^2}{100})$	M_2 / $(\frac{qL^2}{100})$	w / $(\frac{qL^4}{100D})$	M_1 / $(\frac{qL^2}{100})$	M_2 / $(\frac{qL^2}{100})$
2 x 2	0.55685	1.1805	0.5400	0.55530	1.1809	0.5376
4 x 4	0.43840	1.8141	0.8898	0.43670	1.8052	0.8864
8 x 8	0.42499	1.9181	1.0555	0.42064	1.9105	1.0494
16 x 16	0.42124	1.9355	1.1072	0.41560	1.9203	1.0916
32 x 32	0.42178	1.9440	1.1263	0.41363	1.9209	1.1008
T3L	0.41959	1.9366	1.1212	0.41273	1.9178	1.0100
Q4L	0.42695	1.9618	1.1488	0.42352	1.9528	1.1402
T1	0.40383	1.8897	1.0701	0.36156	1.7689	0.9153

Table 11: Simply supported skew plate (soft boundary): displacement and moments at the center. Thick plate: $L/h = 100$. Thin plate: $L/h = 1000$.

	Energy			
Mesh	Q4-LIM	T3L	Q4L	T1
2 x 2	0.378061	0.383241	0.285103	0.115755
4 x 4	0.264296	0.267398	0.256943	0.199369
8 x 8	0.258060	0.261721	0.261289	0.218921
16 x 16	0.261022	0.262122	0.262455	0.239899
32 x 32	0.262519	0.262921	0.262708	0.252967
Ref. [5]	0.265868	0.265868	0.265868	0.265868

Table 12: Simply supported skew plate: energy test. $L/h = 100$ (soft boundary).

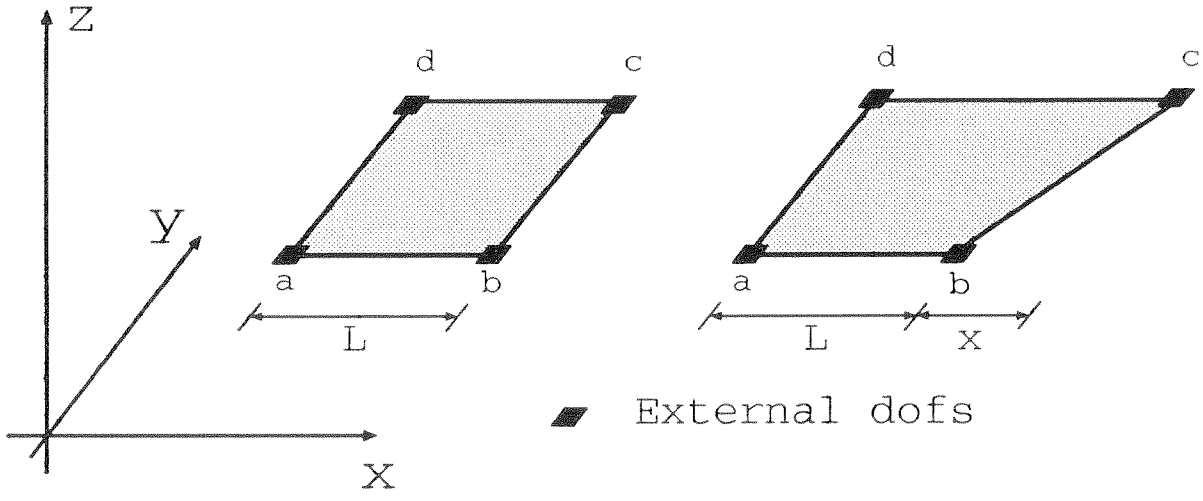

Figure 1: Single element patch test: regular and irregular meshes.

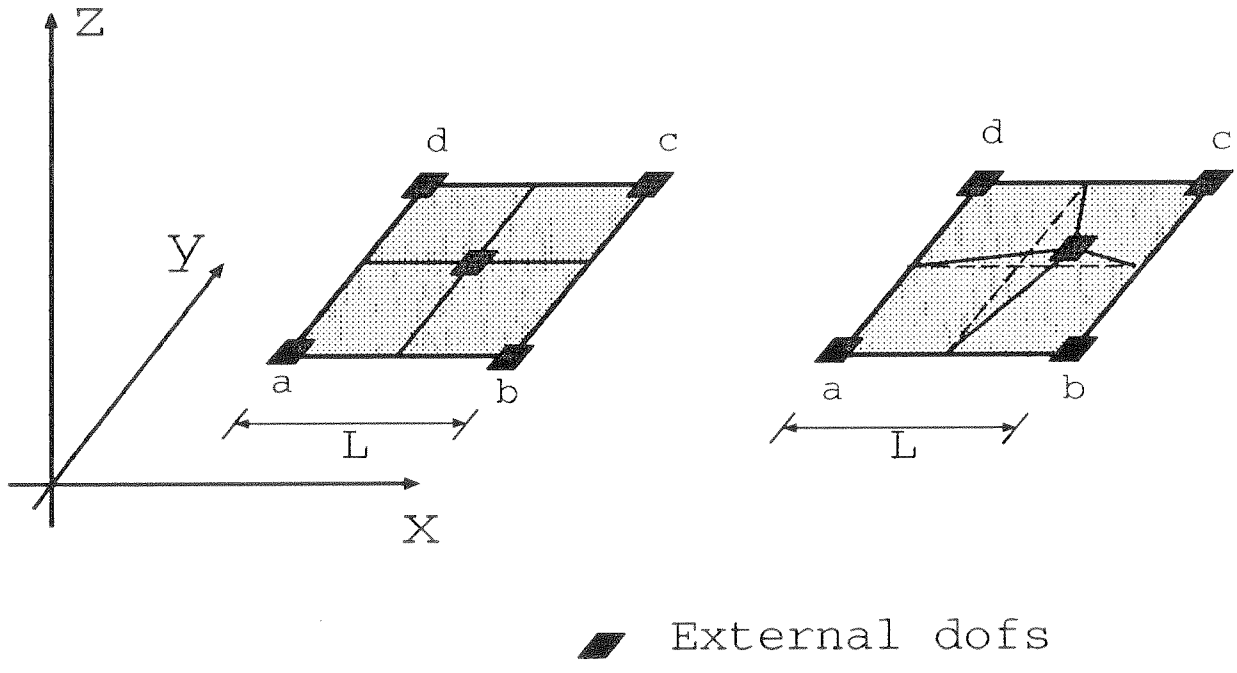

Figure 2: Multi element patch test: regular and irregular meshes.

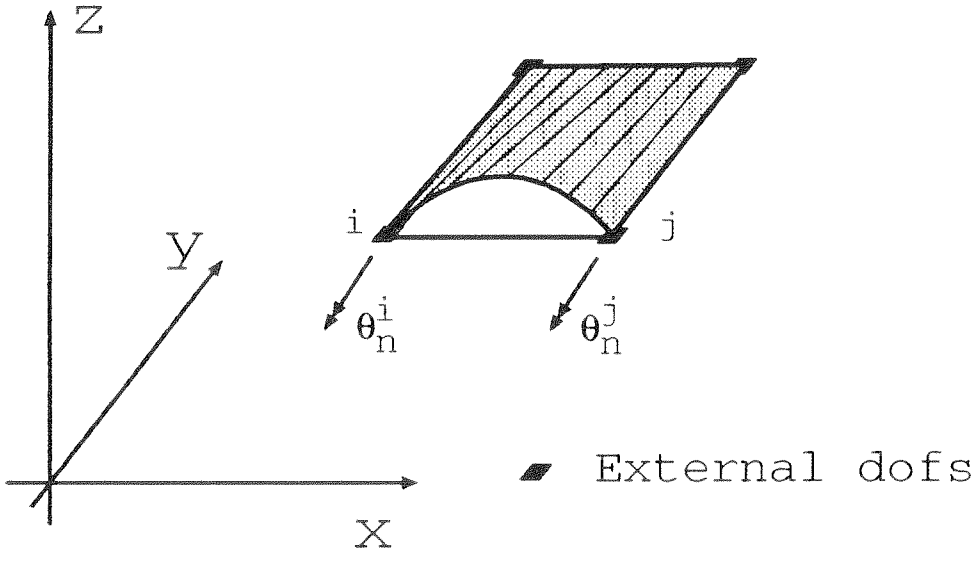

Figure 3: Linked shape function $\mathbf{N}_{w\theta}$ along the i-j side.

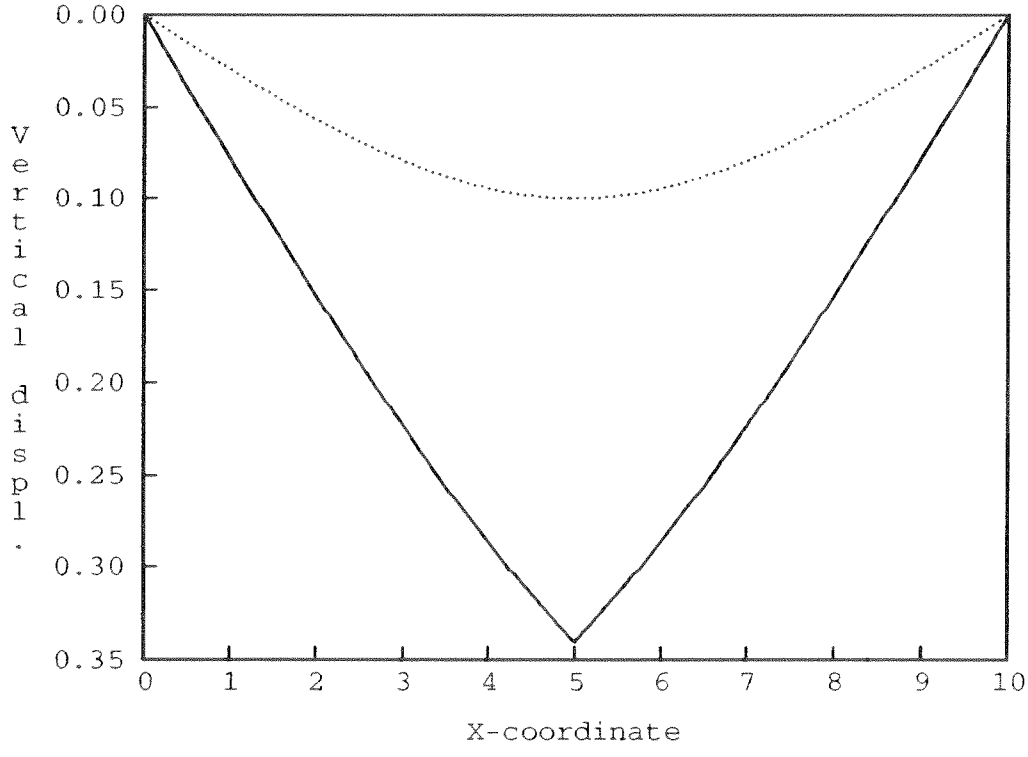

Figure 4: Simply supported beam. Vertical displacement for the beam with shear energy (continuous line) and without shear energy (dotted line).

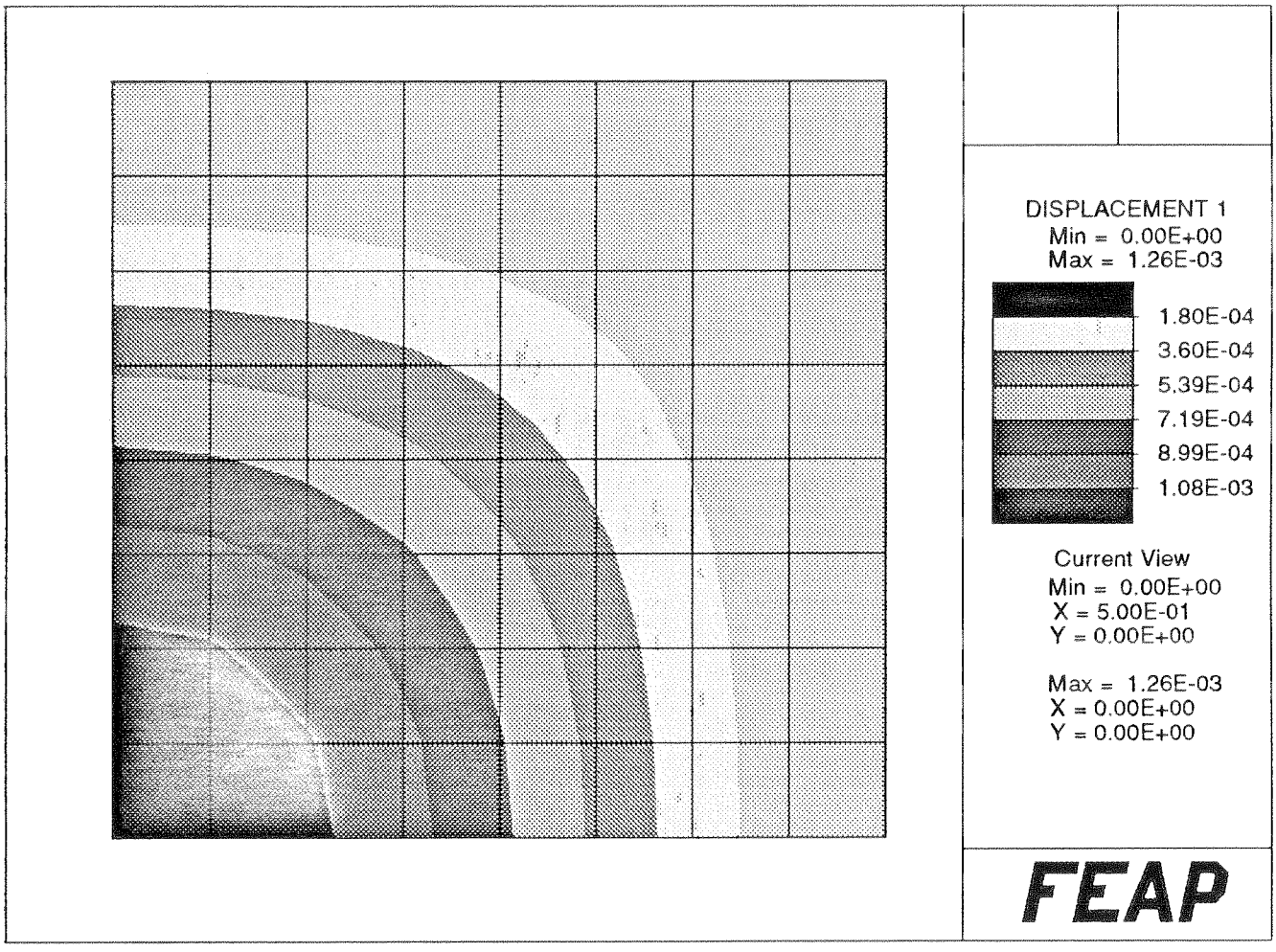

Figure 5: 8×8 mesh for square plate. Only one quarter of the plate (upper right) is considered; the contour of the vertical displacement for the case of clamped boundary condition is plotted.

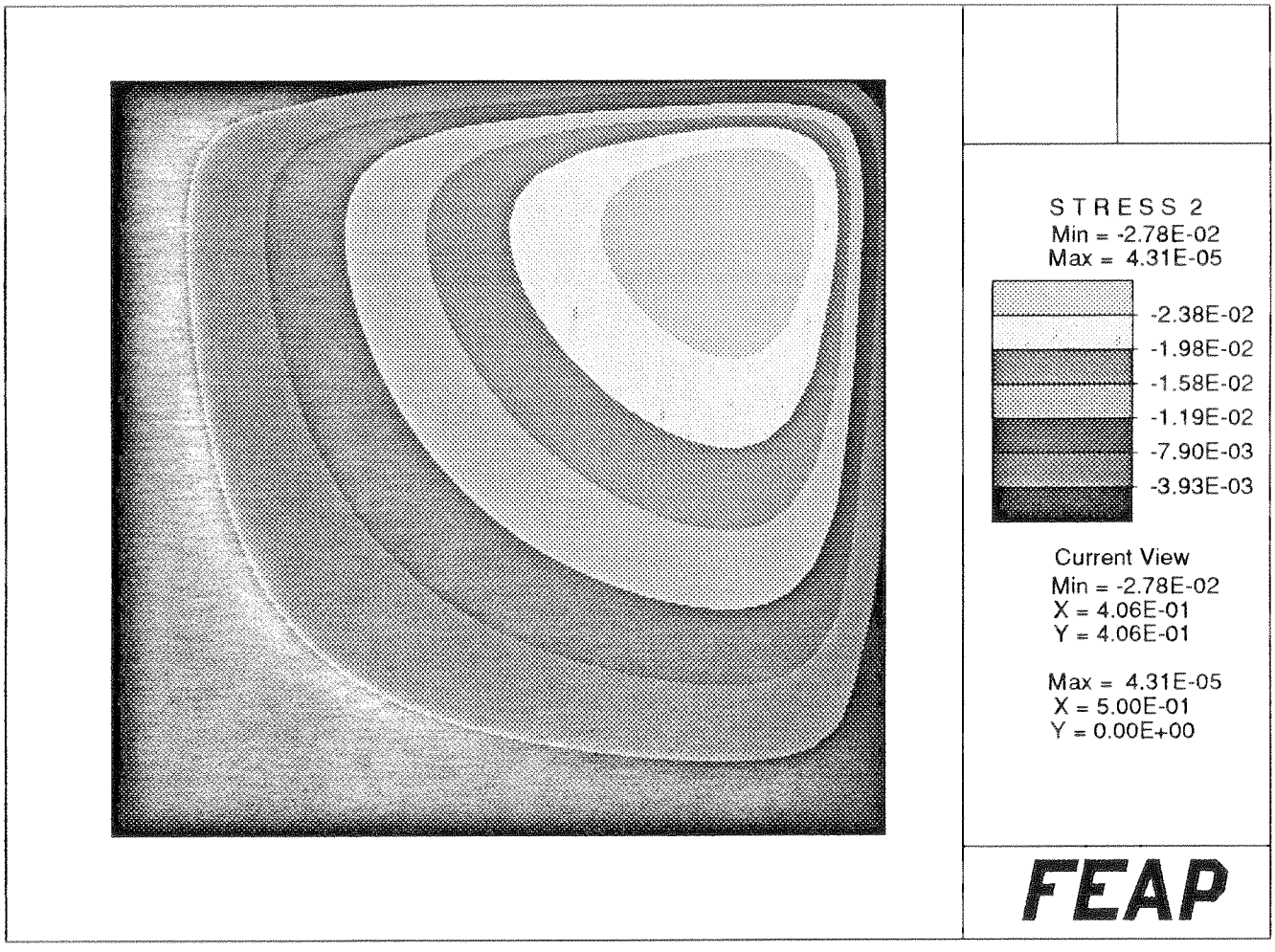

Figure 6: Thick simply supported (SS-1) plate: M_{xy} moment. Only one quarter of the plate (upper right) is considered.

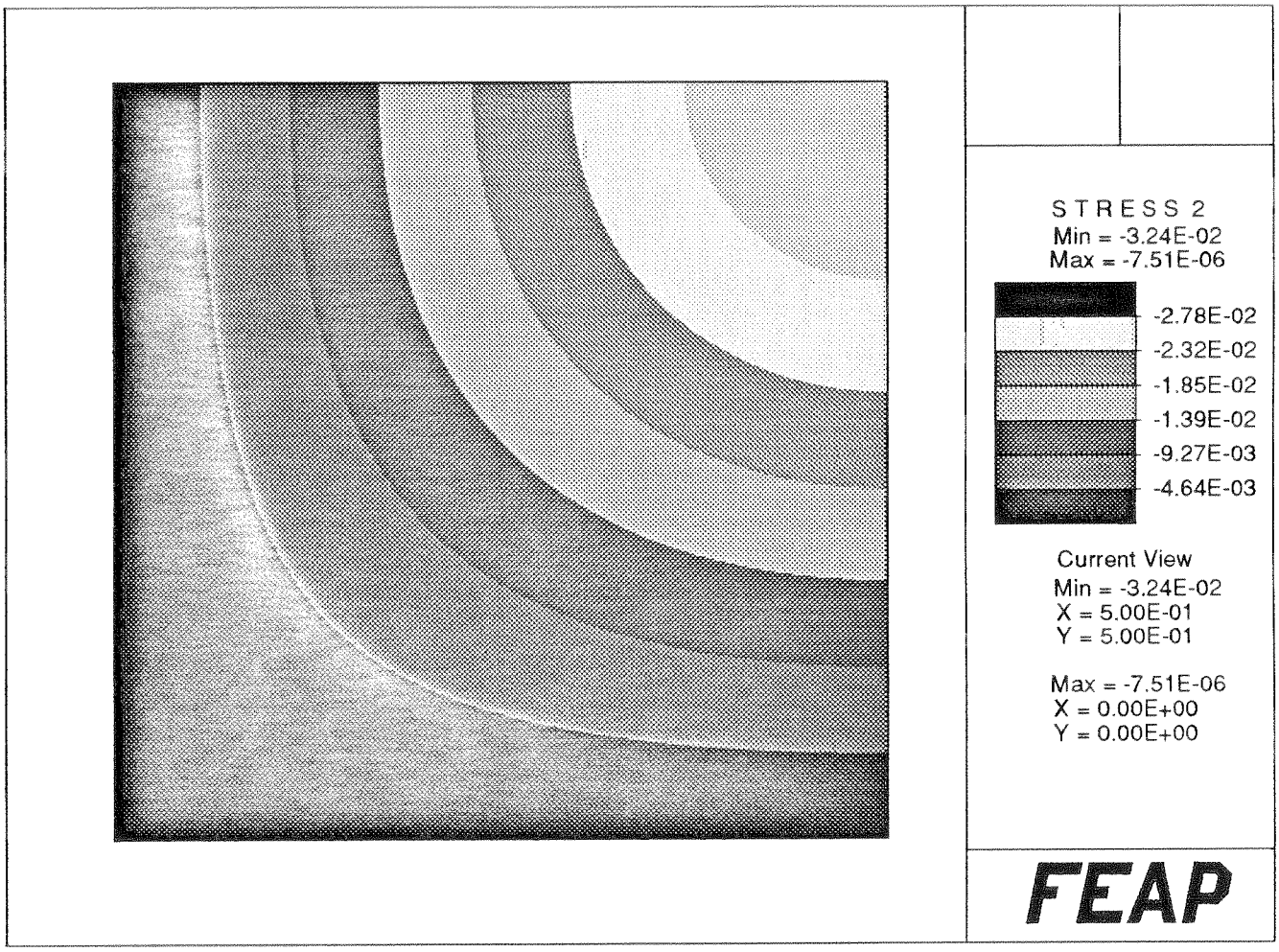

Figure 7: Thick simply supported (SS-2) plate: M_{xy} moment. Only one quarter of the plate (upper right) is considered.

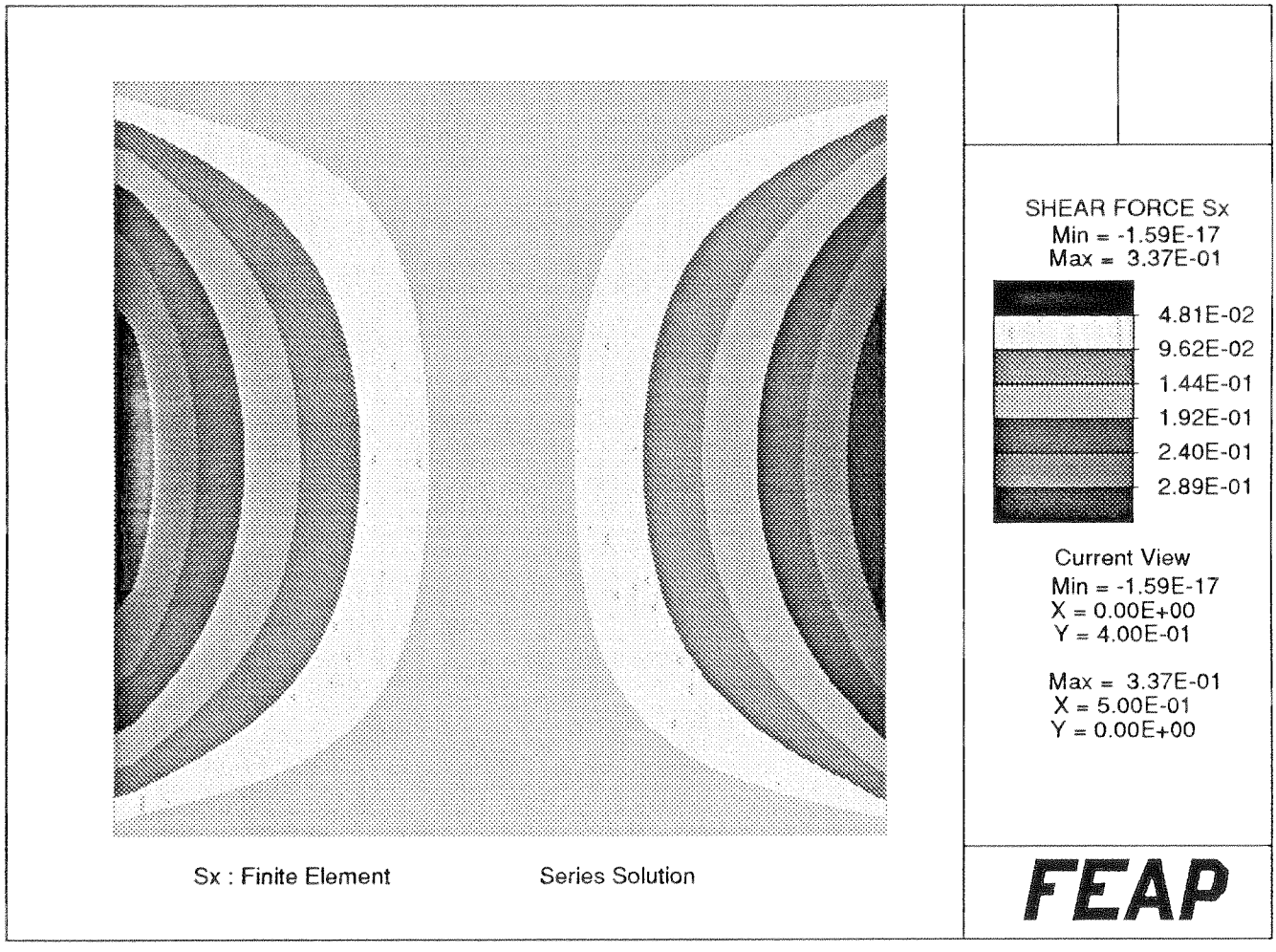

Figure 8: Thin simply supported (SS-2) plate: S_x shear. Finite element solution (left side) versus series solution (right side). The whole plate is plotted.

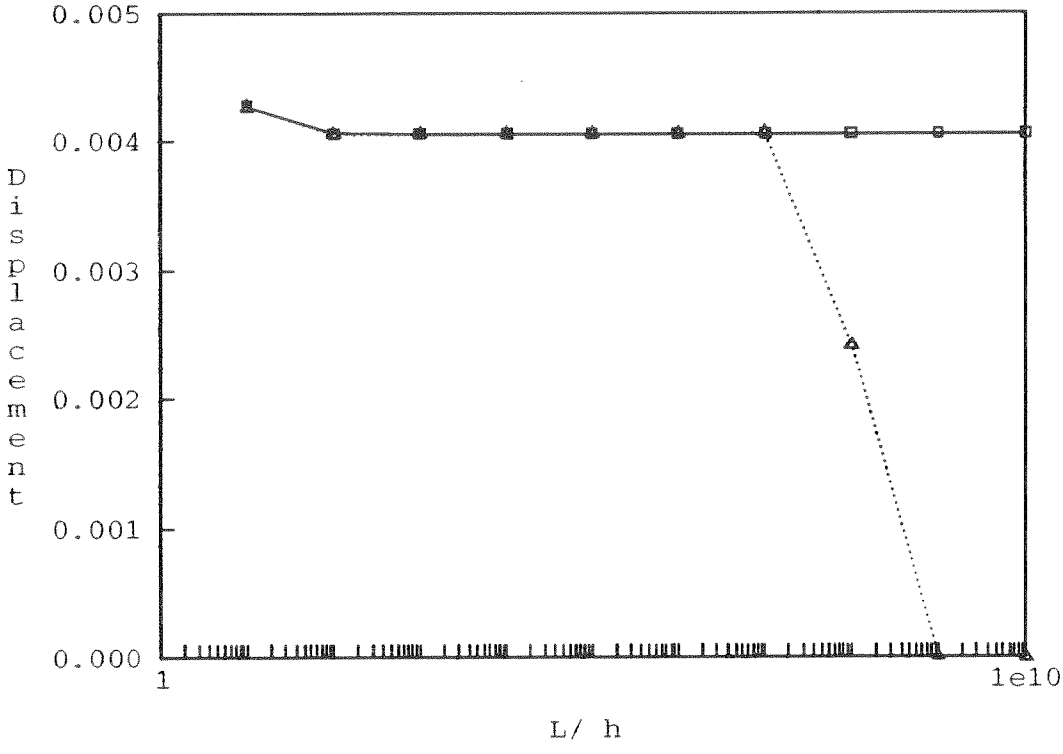

Figure 9: Simply supported (SS-2) plate: displacement versus h/L. The results from the Q4-LIM element are represented with a continuous line; the results from the T1 element are represented with a dotted line.

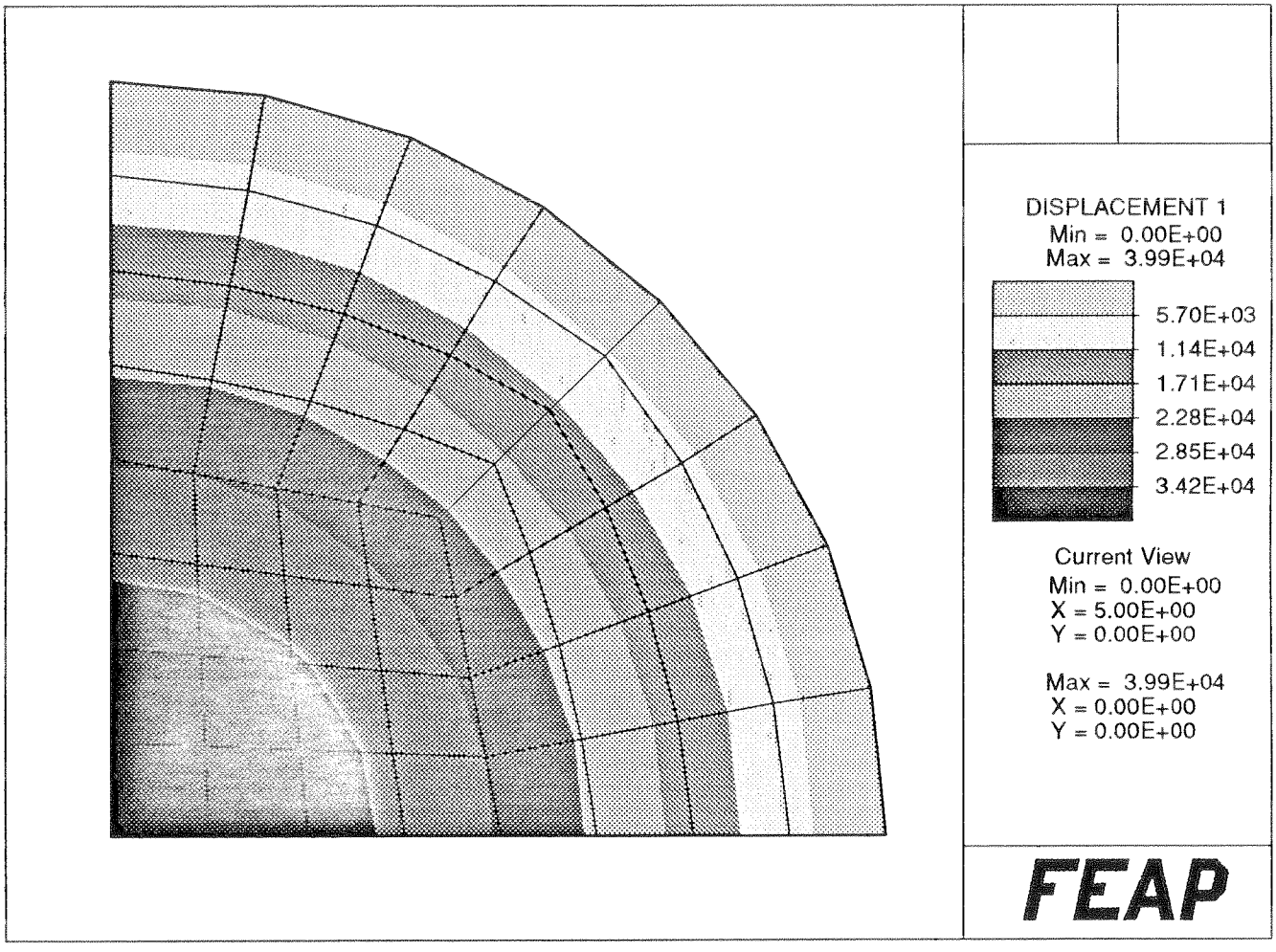

Figure 10: 16-element mesh for simply supported circular plate. Only one quarter of the plate (upper right) is considered and the contour of the vertical displacement is plotted.

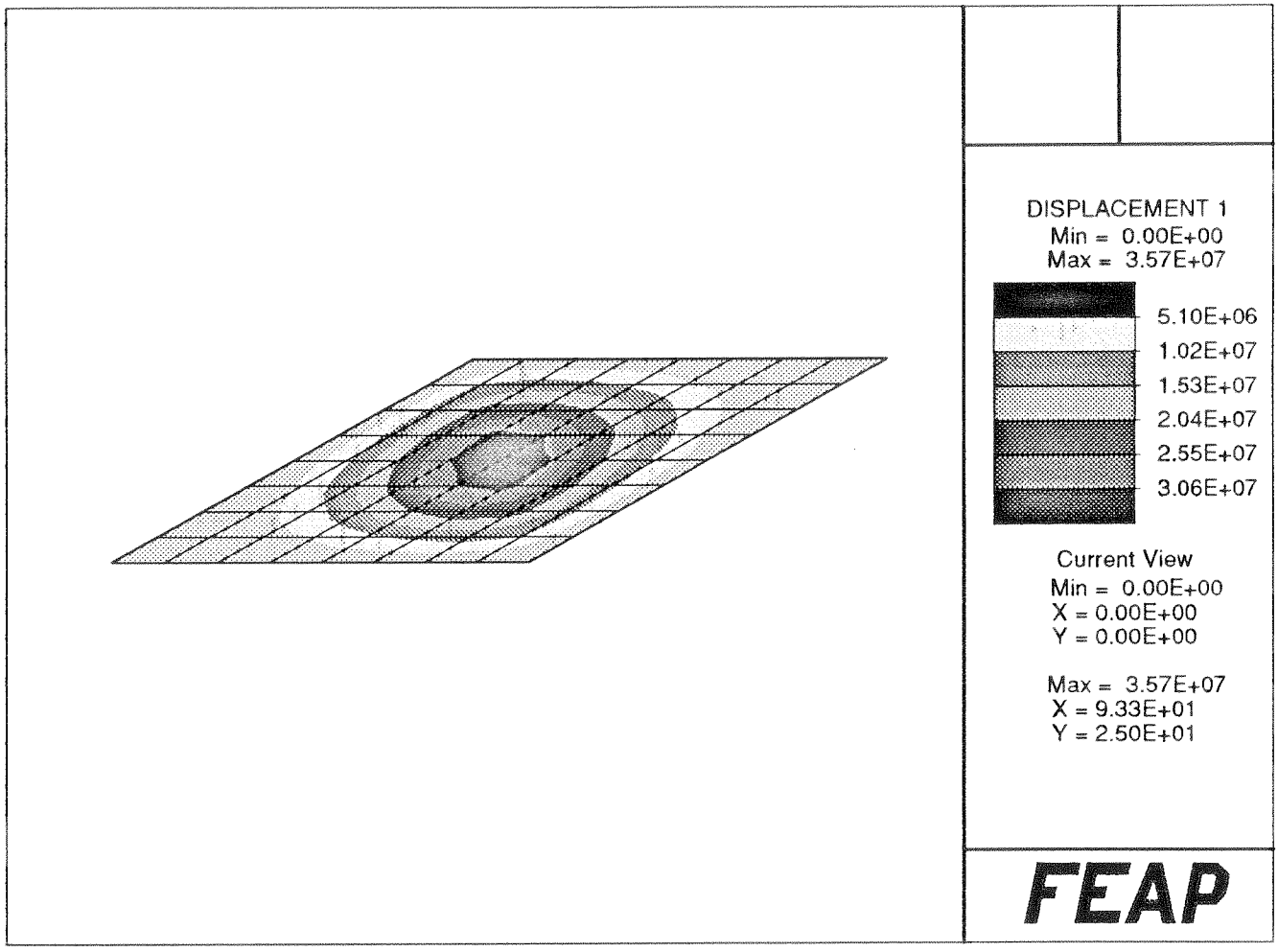

Figure 11: 8×8 mesh for simply supported skew plate. The contour of the vertical displacement is plotted.

List of Figures

List of Tables